Thermodynamics and elastic properties of Ta from first-principles calculations*

Li Qiang(李 强)[a], Huang Duo-Hui(黄多辉)[a], Cao Qi-Long(曹启龙)[a], Wang Fan-Hou(王藩侯)[a]†, Cai Ling-Cang(蔡灵仓)[b], Zhang Xiu-Lu(张修路)[b], and Jing Fu-Qian(经福谦)[b]

[a] *Computational Physics Key Laboratory of Sichuan Province, Yibin University, Yibin* 644000, *China*

[b] *Key Laboratory of National Defense Science and Technology for Shock Wave and Detonation Physics and the Science, Mianyang* 621900, *China*

(Received 25 February 2012; revised manuscript received 19 June 2012)

Within the framework of the quasiharmonic approximation, the thermodynamics and elastic properties of Ta, including phonon density of states (DOS), equation of state, linear thermal expansion coefficient, entropy, enthalpy, heat capacity, elastic constants, bulk modulus, shear modulus, Young's modulus, microhardness, and sound velocity, are studied using the first-principles projector-augmented wave method. The vibrational contribution to Helmholtz free energy is evaluated from the first-principles phonon DOS and the Debye model. The thermal electronic contribution to Helmholtz free energy is estimated from the integration over the electronic DOS. By comparing the experimental results with the calculation results from the first-principles and the Debye model, it is found that the thermodynamic properties of Ta are depicted well by the first-principles. The elastic properties of Ta from the first-principles are consistent with the available experimental data.

Keywords: first-principles, Ta, thermodynamics, Debye model, elastic properties

PACS: 71.15.Mb, 05.70.–a, 81.40.Jj **DOI:** 10.1088/1674-1056/21/12/127102

1. Introduction

Ta-based alloys[1−3] have increasingly attracted attention and been used as high technology materials in recent years, owing to their high chemical and mechanical stabilities and high melting points. In this situation it is necessary to investigate the thermodynamics and elastic properties of Ta. The first-principles calculations, requiring only knowledge of the atomic species and crystal structures and well predicting various properties, including optical properties, thermodynamics, and elastic properties,[4−7] have been selected for the purpose.

In this paper, based on the quasiharmonic approximation, the thermodynamics and elastic properties of Ta are investigated by the first-principles projector-augmented wave method. The phonon DOS, equation of state, linear thermal expansion coefficient, entropy, enthalpy, heat capacity, elastic constants, bulk modulus, shear modulus, Young's modulus, microhardness, and sound velocity of Ta are reported and discussed.

The rest of the present paper is organized as follows. The theoretical methods and the details of the first-principles calculations are shown in Section 2 and Section 3, respectively. In Section 4, the calculation results are given and discussed. Finally, the conclusions are drawn from the present study in Section 5.

2. Theoretical methods

2.1. Quasiharmonic approximation

In combination with the first-principles calculations, thermodynamic behaviours of the solid phase at different temperatures can be described accurately in terms of quasiharmonic approximation.[8−16] Within the framework of the quasiharmonic approach, Helmholtz free energy $F(V,T)$ at volume V and temperature T is usually given by

$$F(V,T) = E(V) + F_{\rm el}(V,T) + F_{\rm vib}(V,T), \quad (1)$$

where $E(V)$ represents the static energy without zero-point vibrational energy from the first-principles total energy calculations at 0 K and volume V; $F_{\rm el}(V,T)$

*Project supported by the Foundation of Key Laboratory of National Defense Science and Technology for Shock Wave and Detonation Physics and the Science and Research Foundation of Sichuan Educational Committee, China (Grant No. 09ZC048).

†Corresponding author. E-mail: wslypq@126.com

© 2012 Chinese Physical Society and IOP Publishing Ltd

is the electronic free energy with respect to the corresponding V and T, which comes from electronic energy due to thermal electronic excitations at the Fermi level; $F_{\rm vib}(V,T)$ is the vibrational free energy.

In the present work, the thermodynamic behaviours of Ta from the first-principles and the Debye model and the elastic properties from the first-principles will be studied based on Eq. (1), wherein $F_{\rm el}(V,T)$ has not been considered in the Debye model.

2.2. Equation of state

The calculated static energies by the first-principles with respect to the volume are fitted to the fourth-order Birch–Murnaghan equation,[17]

$$E(V) = a + bV^{-2/3} + cV^{-4/3} + dV^{-2}. \quad (2)$$

The relationship[17] between pressure P and volume V can be obtained via

$$P = 3B_0 f_{\rm E}(1+2f_{\rm E})^{5/2}\left[1+\frac{3}{2}(B'-4)f_{\rm E} + \frac{3}{2}\left(B_0B'' + (B'-4)(B'-3) + \frac{35}{9}\right)f_{\rm E}^2\right], \quad (3)$$

$$P(V) = -\frac{{\rm d}E}{{\rm d}V}, \quad (4)$$

where

$$B_0 = -V_0\frac{{\rm d}^2E}{{\rm d}V^2}, \quad f_{\rm E} = [(V/V_0)^{2/3}-1]/2,$$
$$B' = \frac{\partial B}{\partial P}, \quad B'' = \frac{-1}{B_0}[(3-B')(4-B') + \frac{35}{9}.$$

2.3. Vibrational contribution to the Helmholtz free energy

2.3.1. Vibrational free energy from the first-principles

Based on the phonon DOS $g(\omega)$, vibrational free energy from the first-principles can be written as follows:[8,15]

$$F_{\rm vib}(V,T) = k_{\rm B}T\int_0^\infty \ln\left[2\sinh\frac{\hbar\omega}{2k_{\rm B}T}\right]g(\omega){\rm d}(\omega), \quad (5)$$

where ω and $\hbar$ are the phonon frequency and the reduced Planck constant, respectively.

2.3.2. Vibrational free energy from the Debye model

Vibrational free energy can be calculated by the empirical Debye model as follows:[18]

$$F_{\rm vib}(\Theta,T) = nkT\left[\frac{9}{8}\frac{\Theta}{T} + 3\ln(1-{\rm e}^{-\Theta/T}) - D(\Theta/T)\right], \quad (6)$$

where $D(\Theta/T)$ is the Debye function. Debye temperature can be given by[18]

$$\Theta = \frac{\hbar}{K}[6\pi^2V^{1/2}n]^{1/3}f(\sigma)\sqrt{\frac{B_{\rm s}}{M}}, \quad (7)$$

$$B_{\rm S} \approx B_{\rm static}(V) \approx B_{\rm static}(V_{\rm opt}) = V\left(\frac{{\rm d}^2E(V)}{{\rm d}V^2}\right), \quad (8)$$

where M is the molecular mass per unit cell; $B_{\rm s}$ is the adiabatic bulk modulus,[19] which is approximated by the static compressibility; σ is the Poisson's ratio and has a value of 0.25; $f(\sigma)$ can be obtained by[20]

$$f(\sigma) = \left\{3\left[2\left(\frac{2}{3}\frac{1+\sigma}{1-2\sigma}\right)^{3/2} + \left(\frac{1}{3}\frac{1+\sigma}{1-\sigma}\right)^{3/2}\right]^{-1}\right\}^{1/3}. \quad (9)$$

The non-equilibrium Gibbs function $G^*(V;P,T)$ can be minimized with respect to volume V

$$\left(\frac{\partial G^*(V;P,T)}{\partial V}\right)_{P,T} = 0. \quad (10)$$

The heat capacity C_V is estimated by[18]

$$C_V = 3nk\left[4D(\Theta/T) - \frac{3\Theta/T}{{\rm e}^{\Theta/T}-1}\right]. \quad (11)$$

Based on the quasiharmonic Debye model, the thermodynamic parameters of Ta at any pressure and temperature can be estimated from the calculated $E(V)$ data at $T = 0$ K and $P = 0$ GPa.

2.4. Electronic free energy from the first-principles

The quantity $F_{\rm el}(V,T)$ is very important for a metal system and can be given by Mermin statistics $F_{\rm el}(V,T) = E_{\rm el}(V,T) - TS_{\rm vib}(V,T)$, where $E_{\rm el}(V,T)$ is the internal energy with respect to the corresponding V and T, and $S_{\rm vib}(V,T)$ is the electronic entropy. The quantity $E_{\rm el}(V,T)$ can be written as[8]

$$E_{\rm el}(V,T) = \int n(\varepsilon)f\varepsilon{\rm d}\varepsilon - \int^{\varepsilon_{\rm F}} n(\varepsilon)\varepsilon{\rm d}\varepsilon, \quad (12)$$

where $n(\varepsilon)$ is the electronic DOS, ε is the energy eigenvalue, $\varepsilon_{\rm F}$ is Fermi energy, f is the Fermi–Dirac distribution function. The electronic entropy is given by[8]

$$S_{\rm el}(V,T) = -k_{\rm B}\int n(\varepsilon)\left[f\,\ln f + (1-f)\,\ln(1-f)\right]{\rm d}\varepsilon, \quad (13)$$

where $k_{\rm B}$ is the Boltzmann constant.

2.5. Elastic constants by strain versus stress method

A method was proposed for calculating elastic constant as a function of temperature in previous literature.[21] Ignoring the anharmonic effect and the fluctuation of microscopic stress tensor, the elastic constants $C_{ij}(T)$ can be evaluated by volume change as follows. The elastic constants $C_{ij}(V)$ corresponding to different equilibrium volumes can be calculated at 0 K from the first-principles. According to the quasi-harmonic approach, volume change $V(T)$ as a function of temperature is predicted from the phonon calculations. Based on the predicted $C_{ij}(V)$ and $V(T)$ mentioned above, temperature-dependent elastic constants $C_{ij}(T)$ each are a function of V.

To calculate the elastic constants, the efficient stress–strain method proposed by Shang *et al.*[21] is employed in the present work. If a set of strains can be given by

$$\varepsilon = (\varepsilon_1\varepsilon_2\varepsilon_3\varepsilon_4\ \varepsilon_5\varepsilon_6), \tag{14}$$

where ε_1, ε_2, and ε_3 are the normal strains and the others are shear strains. Lattice vector R is written as

$$R = \begin{pmatrix} a_1 & a_2 & a_3 \\ b_1 & b_2 & b_3 \\ c_1 & c_2 & c_3 \end{pmatrix}, \tag{15}$$

where a_i, b_i, and c_i are the components of lattice vector R. The six strains will be imposed on the origin lattice vector R and the new lattice vector R' can be obtained from

$$R' = R \begin{pmatrix} 1+\varepsilon_1 & \varepsilon_6/2 & \varepsilon_5/2 \\ \varepsilon_6/2 & 1+\varepsilon_2 & \varepsilon_4/2 \\ \varepsilon_5/2 & \varepsilon_4\ /\ 2 & 1+\varepsilon_3 \end{pmatrix}. \tag{16}$$

A set of stresses $\sigma = (\sigma_1\sigma_2\ \sigma_3\sigma_4\sigma_5\sigma_6)$ is generated because of the crystal deformation from strains ε_i. Thus, the elastic constants are determined by Hooke's law

$$\sigma = C_{ij}\varepsilon, \tag{17}$$

where C_{ij} is the 6×6 elastic constant matrix. The quantities σ and ε are the stress and strain matrix, respectively. In the present work, n sets of strains will be required to calculate elastic constants.

For the cubic Ta, the elastic constant matrix is

$$C_{ij} = \begin{pmatrix} C_{11} & C_{12} & C_{13} & 0 & 0 & 0 \\ C_{22} & C_{23} & 0 & 0 & 0 & \\ C_{33} & 0 & 0 & 0 & & \\ C_{44} & 0 & 0 & & & \\ C_{55} & 0 & & & & \\ C_{66} & & & & & \end{pmatrix}, \tag{18}$$

where the lower-left part of C_{ij} is omitted. The cubic crystal of Ta has three independent elastic constants C_{11}, C_{12}, and C_{44}.

The theoretical elastic properties, including bulk modulus, shear modulus, Young's modulus, and microhardness, can be determined from the independent elastic constants $C_{ij}(T)$. The average isotropic bulk modulus (B), shear modulus (G), Yong's modulus ($Y_{\rm m}$), and microhardness ($H_{\rm V}$) have been calculated according to Voigt–Reuss–Hill approximations as shown below[22,23]

$$B = B_{\rm V} = B_{\rm R} = (C_{11} + 2C_{12})/3, \tag{19}$$

$$\begin{aligned} G &= G_{\rm V} + G_{\rm R} \\ &= (C_{11} - C_{12} + 3C_{44})/5 \\ &\quad + 5(C_{11} - C_{12})C_{44}/[4C_{44} + 3(C_{11} - C_{12})], \end{aligned} \tag{20}$$

$$Y_{\rm m} = 9BG/(3B + G), \tag{21}$$

$$H_{\rm V} = (1 - 2\sigma)Y_{\rm m}/[6(1 + \sigma)], \tag{22}$$

where the Poisson's ratio (σ) is calculated by $\sigma = (3B - 2G)/(6B + 2G)$. Voigt's approach gives the upper bound of elastic properties in terms of the uniform strain. Reuss's approach gives the lower bound in terms of the uniform strain. Hill's approach[22] gives the average value of Voigt and Reuss.

The averaged aggregate velocities from the calculated bulk modulus and shear modulus can be achieved as follows:[24]

$$V_{\rm p} = \left[(B + 4/3G)/\rho\right]^{1/2}, \tag{23}$$

$$V_{\rm s} = (B/\rho)^{1/2}, \tag{24}$$

where $V_{\rm P}$ and $V_{\rm S}$ are the longitudinal and shear sound velocities, respectively.

3. Details of the first-principles calculations

The density functional theory (DFT) calculations are performed based on the *ab initio* simulation package (VASP).[25] The electron–ion interactions

are treated within the projector-augmented wave.[26] The exchange correlation potential is described by generalized gradient approximation of PW91.[27] The Brillouin zone (BZ) is sampled by a 27×27×27 Monkhorst–Pack[28] mesh of k points for Ta. The electronic wave functions are expanded in a plane wave basis set with energy cut-off of 360 eV. Allowed error in total energy is smaller than 10^{-4} eV per atom between two electronic self-consistent steps. The change in the total free energy is smaller than -10^{-3} eV per atom between two ionic step relaxations.

The phonon DOS calculations are carried out by a direct force constant method, which is a feasible method of calculating the vibrational properties from the first principles based on the quasiharmonic approximation, as implemented in ATAT code.[29] We use the 27-atom super-cell for Ta. The electronic free energy is obtained using the Felec code in ATAT code, in which the Fermi–Dirac function is chosen for the smearing of the k-point grid.

4. Results and discussion

4.1. Equation of state

The predicted volume of Ta as a function of pressure is compared with experimental data,[30,31] four-parameter equation of state,[32] and other first-principles calculations,[9] which are shown in Fig. 1, together with the energy versus volume relation from the first-principles (in the inset). From Fig. 1, the fitted pressure–volume relation obtained through the fourth-order Birch–Murnaghan equation accords reasonably with the diamond-anvil cell (DAC) experimental results and the calculation results from four-parameter equation of state and other first-principles.

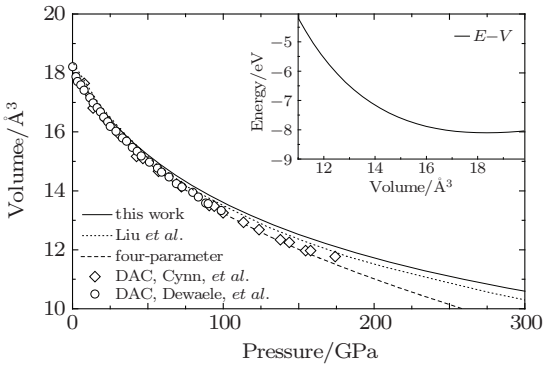


Fig. 1. Curves of volume versus pressure for Ta, obtained from DAC experiments, four-parameter equation of state, and other calculations; energy–volume relation obtained from the first-principles shown in the inset.

The lattice parameter a_0, bulk modulus B_0, and its first derivative B_0', which are all calculated by the fourth-order Birch–Murnaghan equation of Ta, are 3.315 Å, 196.9 GPa, and 3.62, respectively, which are in good agreement with the experimental values (3.305 Å,[33] 196.3 GPa,[34] and 3.52[32]).

4.2. Thermodynamic properties of Ta

The phonon DOS of Ta at 0 GPa is obtained from the first-principles calculations. Figure 2 shows the calculated phonon DOS of Ta together with the experimental measurements[35] by neutron diffractions and other first-principles calculations.[9] From Fig. 2, it is found that our obtained phonon DOS of Ta and the results by Liu *et al.* are consistent with the measurements at low frequency, but slight deviations can be observed at high frequency, which are mainly due to the current calculation based on harmony approximation at 0 K, while the experimental measurements are performed at 296 K and the anharmonic effect could be induced by the higher temperature.

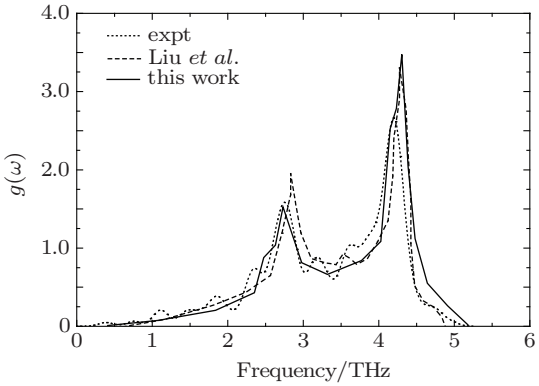


Fig. 2. Calculated phonon DOSs versus frequency for Ta at theoretical equilibrium volume, compared with experimental data and other calculations.

Figure 3 shows the temperature-dependent heat capacities of Ta at the equilibrium volume obtained by the phonon DOS and the Debye model. As a result, the heat capacities at constant volume from the first-principles and the Debye model increase dramatically as temperature increases and finally approach the Dulong–Petit result $3nN_{\rm A}k_{\rm B}$. With the increase of temperature, the thermal electronic contribution to Helmholtz free energy increases. The Debye temperature of Ta calculated by Eq. (6) is 269 K, which is consistent with the experimental value around 261.9 K.[36]

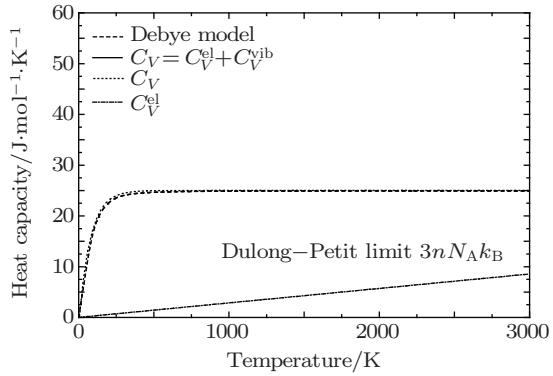


Fig. 3. Heat capacities at constant volume for Ta versus temperature, calculated by the first-principles and the Debye model.

The linear thermal expansion coefficient α at 0 GPa can be obtained via

$$\alpha = \frac{1}{3V}\left(\frac{\partial V}{\partial T}\right)_P, \tag{25}$$

where V is the equilibrium volume corresponding to the temperature of interest at 0 GPa. Figure 4 illustrates the linear thermal expansion coefficient with respect to the temperature at 0 GPa, calculated by the first-principles and the Debye model, together with experimental results and other calculations. Electronic contributions are considered in the first-principles calculations for all the thermal properties discussed in this section. It can be noted that the linear thermal expansion coefficients from the calculations of the first-principles and the Debye model increase rapidly with the increase of temperature below 250 K. The predicted linear thermal expansion coefficients from the first-principles accord well with the experimental measurements[37] and the latest theoretic data[9,38] in a range from 0 to 3000 K. In contrast, the estimated values from the Debye model deviate from the present first-principles calculations and the latest theoretic data. The results given by Cohen and Gülseren[39] from the particle-in-cell (PIC) model are relatively far from experimental results.

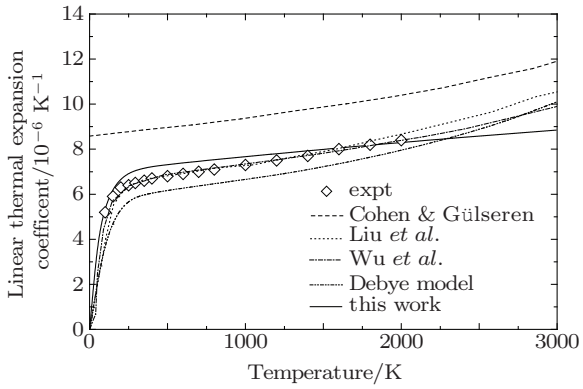


Fig. 4. Linear thermal expansion coefficients versus temperature for Ta, calculated by the first-principles and the Debye model, respectively, compared with experimental data and other calculations.

The entropies of Ta, calculated by the first-principles and Debye model, are shown in Fig. 5, where the entropy is given by $S = -(\partial F/\partial T)_P$ under 0 GPa. The experimental entropies[39] with respect to the corresponding temperature are also shown in Fig. 5 for comparison. From Fig. 5, it can be observed that the entropies of Ta calculated by the first-principles are more accurate than the ones calculated by the Debye model. Our results from the Debye model are in agreement with those given by Wu *et al.*,[38] in which the same principle was used.

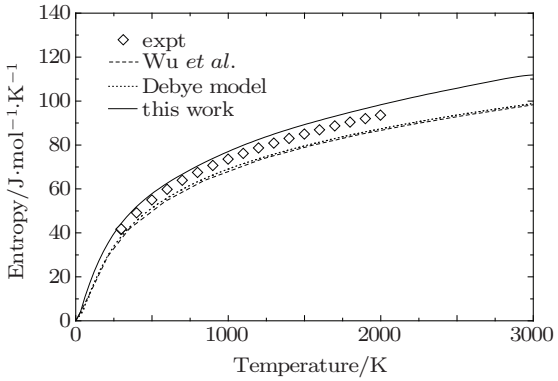


Fig. 5. Entropies at constant pressure versus temperature for Ta, calculated by the first-principles and the Debye model, respectively, compared with experimental data and other calculations.

Figure 6 illustrates the enthalpies of bcc Ta, obtained by the first-principles and the Debye model, together with the thermochemical data versus temperature,[39] where the enthalpy at 0 GPa is obtained by $H = F + TS$. It is obvious that the entropies of Ta calculated by the first-principles accord well with the experimental values.

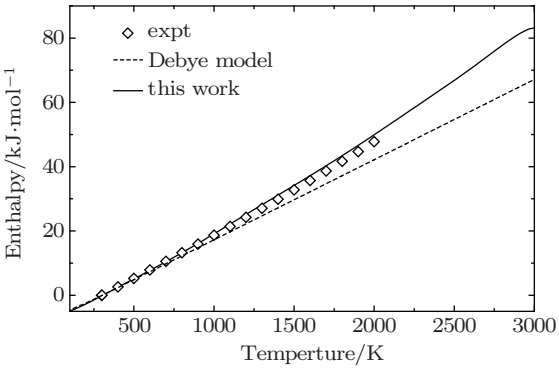


Fig. 6. Enthalpies versus temperature for Ta, calculated by the first-principles and the Debye model, respectively, together with the experiment values (open diamond).

The heat capacity at constant pressure from the first-principles is described by $C_{\rm p} = (\partial H/\partial T)_P$, where H represents the enthalpy at constant pressure. In Fig. 7, we plot $C_{\rm p}$ versus temperature, calculated by the first-principles and the Debye model, respectively, in comparison with measurements[40] and other calculations.[9,38,39] The heat capacities at constant pressure $C_{\rm p}$ from the first-principles and the Debye model increase rapidly below 300 K as temperature increases. The first-principles predicted $C_{\rm p}$ in a range from 300 K to 500 K is closer to the experimental data and the results presented by Liu *et al.*[9] than that obtained from the Debye model. The results given by Cohen and Gülseren[39] deviate from our results and the latest theoretic results.[9,38]

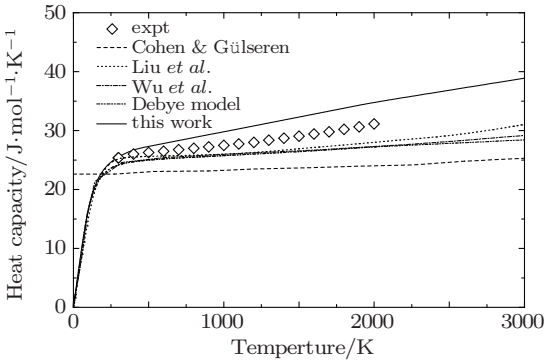


Fig. 7. Heat capacities at constant pressure versus temperature for Ta, calculated by the first-principles and the Debye model, respectively, compared with experimental data and other calculations.

As is well known, in the Debye model only the vibrational contribution to Helmholtz free energy is considered, but the thermal electronic contribution is ignored. According to the Debye model, the lattice wave is distinguished from the transverse wave and the longitudinal wave. The dispersion relations of the transverse wave and the longitudinal wave are both linear, which is inconsistent with the actual situations. For metal Ta, with the increase of temperature, the thermal electronic contribution to Helmholtz free energy increases. In the first-principles calculations, both the thermal electronic and the vibrational contribution to Helmholtz free energy are taken into account. The predicted phonon DOS from the first principles is in good accordance with the experimental result as mentioned above. Therefore, the first-principles work is better for thermodynamics of Ta than the Debye model.

4.3. Elastic properties of Ta

The elastic constants of the bcc Ta with respect to the temperature are deduced from the equation $C_{ij}(T) = C_{ij}(T(V))$ and presented in Fig. 8, together with the experimental data. From Fig. 8, the elastic constants (C_{11} and C_{44}) predicted by the first-principles decrease with the increase of temperature, which is consistent with the ultrasonic measurements presented by Featherston and Neighbors[41] and by Walker and Bujard.[42] For C_{12}, the calculated rates decreasing with the temperature increasing from 300 K to 3000 K are slightly larger than those of the experimental data. The discrepancies observed in the C_{12} are maybe due to neglecting the contributions of $F_{\rm vib}(V,T)$ and $F_{\rm el}(V,T)$ to these second derivatives.[43] The exceptionally large elastic constants of Ta in a range from 0 K to 3000 K can be correlated to its high melting point (3250 K) and cohesive energy (8.1 eV).

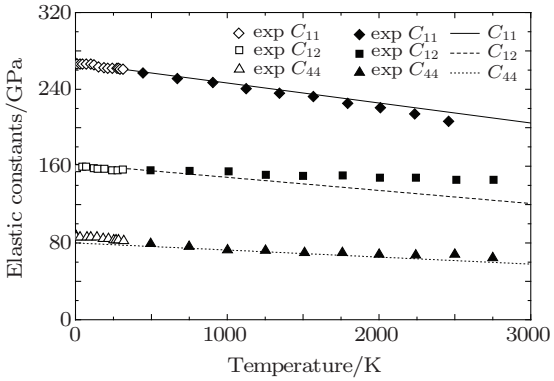


Fig. 8. Elastic constants at constant pressure versus temperature for Ta, calculated by the first-principles, compared with the experimental data.

Figure 9 shows the first-principles calculated elastic properties of Ta at different temperatures, including bulk modulus, shear modulus, and Young's modulus, together with the experiment values.[34] The predicted bulk modulus B is 193.6 GPa at 298 K, which accords well with the measured result ($\sim$ 196.3 GPa). The calculated shear modulus G is 66.0 GPa at room temperature, well consistent with the measured value ($\sim$ 69.2 GPa). The calculated Young's modulus $Y_{\rm m}$ is 178.1 GPa, which is reasonably in agreement with the experimental value ($\sim$ 185.7 GPa). The predicted bulk and Young's modulus of Ta decrease linearly as temperature increases, which implies that the Ta crystal softens with the increase of temperature, thereby making it compressed and lengthened more easily. The shear modulus of Ta reduces 24% from 0 K to

3000 K, which means Ta crystal softens as temperature increases, thereby making the shear deformation appear more easily. It is worth mentioning that Ta crystal has a very high elastic modulus in the range from 0 K to 3000 K.

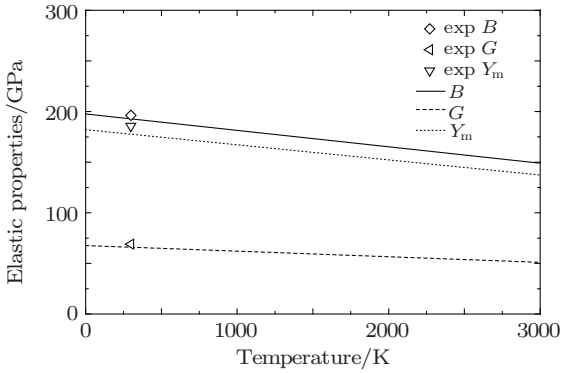


Fig. 9. Elastic properties at constant pressure versus temperature for Ta, calculated by the first-principles, compared with the experiment values at room temperature.

The estimated microhardness values of Ta are shown in Fig. 10. It can be seen that the microhardness at 0 GPa decreases gradually as temperature increases, which indicates that the Ta crystal softens with the increase of temperature, thereby making it compressed more easily. The predicted microhardness is 6.74 GPa at 298 K from the first-principles, which is reasonably in agreement with the experimental data[44] (1.17 GPa∼11.6 GPa).

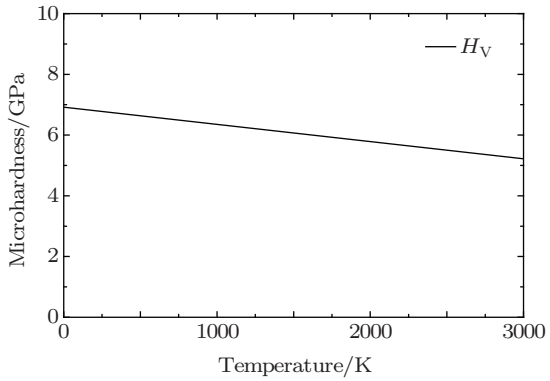


Fig. 10. Microhardness at constant pressure versus temperature for Ta, calculated by the first-principles.

The isotropically average aggregation velocities at different temperatures can be readily obtained from standard relations discussed in Section 2 and are shown in Fig. 11. From Fig. 11, the average aggregation velocities V_p and V_s decrease monotonically as temperature increases, but the V_p dropped off more quickly than the V_s, which implies that the temperature has a large influence on the speed of the longitudinal wave of Ta and the speed of the shear wave is less sensitive to temperature change in the range from 0 K to 3000 K. The predicted average aggregation velocities V_p and V_s are 4.13 km/s and 2.01 km/s at 293 K, respectively, which are consistent with the experimental data[45] (4.15 km/s and 2.04 km/s).

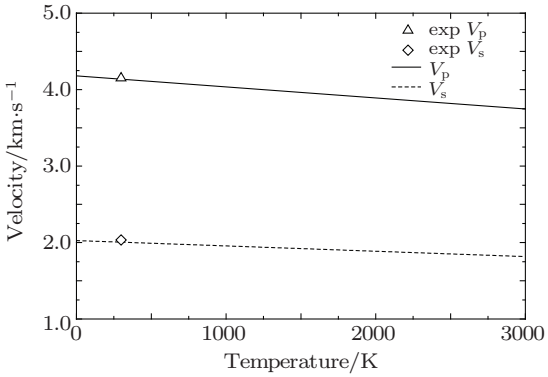


Fig. 11. Aggregate sound velocities (V_p and V_s) versus temperature from the first-principles, compared with the experimental values at room temperature.

5. Conclusion

Based on the quasiharmonic approximation, temperature-dependent thermodynamic properties of Ta, including thermal expansion coefficient, entropy, enthalpy and heat capacity, are studied using the first-principles and the Debye model. The elastic properties of Ta with respect to the temperature at 0 GPa are investigated using the first-principles strain versus stress method. The calculated pressure–volume relation, lattice parameter a_0, bulk modulus B_0, and its first derivative B_0' by the fourth-order Birch–Murnaghan equation of Ta are in agreement with the corresponding experimental values. The phonon DOS from the first-principles is consistent with experimental measurements. Considering the thermal electronic contribution to Helmholtz free energy, the predicted linear thermal expansion coefficients from the first-principles accord well with the experimental measurements in a range from 0 K to 3000 K. The predicted entropies, enthalpies, and heat capacities of Ta from the first-principles are in much better agreement with the experimental values than those from the Debye model. The predicted elastic constants (C_{11} and C_{44}) by the first-principles decrease with the increase of temperature and accord with the ultrasonic measurements. The calculated rates of C_{12} decreasing with increasing temperature are slightly larger than those of the experimental data at high temperatures, which maybe is due to neglecting the contributions of electronic free energy and vibrational free energy

to these second derivatives. The first-principles calculated bulk modulus, shear modulus, Young's modulus, and microhardness all decrease smoothly as temperature increases and accord with the corresponding experimental values at room temperature. The average aggregation velocities predicted from the first-principles decrease monotonically as temperature increases and accord well with the experimental data at room temperature. The temperature has a large influence on the speed of the longitudinal wave of Ta, but the speed of the shear wave is less sensitive to temperature change in the range from 0 K to 3000 K.

References

[1] Lucas M S, Bourne W C and Sheets A O 2011 *Mater. Sci. Eng.* B **176** 1079

[2] Keith J L, Jeremy T B and Steven J Z 2007 *J. Nucl. Mater.* **366** 353

[3] Zhang W, Arai K and Qin C L 2008 *Mater. Sci. Eng.* A **485** 690

[4] Luo F, Fu M, Ji G F and Chen X R 2010 *Chin. Phys.* B **19** 027101

[5] Yang H, Chang J, Li Z and Chen X R 2009 *Chin. Phys.* B **18** 4443

[6] Yu J X, Fu M, Ji G F and Chen X R 2009 *Chin. Phys.* B **18** 269

[7] Zhu J, Yu J X, Wang Y J, Chen X R and Jing F Q 2008 *Chin. Phys.* B **17** 2216

[8] Wang Y, Liu Z K and Chen L Q 2004 *Acta Mater.* **52** 2665

[9] Liu Z L, Cai L C, Chen X R, Wu Q and Jing F Q 2009 *J. Phys.: Condens. Matter* **21** 095408

[10] Arroyave R and Liu Z K 2006 *Phys. Rev.* B **74** 174118

[11] Mohri T and Chen Y 2004 *J. Alloys Compd.* **383** 23

[12] Moruzzi V L, Janak J F and Schwarz K 1988 *Phys. Rev.* B **37** 790

[13] Peng F, Fu H Z and Yang X D 2008 *Solid State Commun.* **145** 91

[14] Shang S and Böttger A J 2005 *Acta Mater.* **53** 255

[15] Shang S L, Wang Y and Liu Z K 2007 *Phys. Rev.* B **75** 024302

[16] Arroyave R, Shin D and Liu Z K 2005 *Acta Mater.* **53** 1809

[17] Murnaghan F D 1937 *Am. J. Math.* **59** 235

[18] Blanco M A, Pendas A M and Francisco E J 1996 *J. Mol. Struct.* (Theochem) **368** 245

[19] Blanco M A, Francisco E and Luana V 2004 *Comput. Phys. Commun.* **158** 7

[20] Francisco E, Recio J M, Blanco M A and Martín P A 1998 *J. Phys. Chem.* **102** 1595.

[21] Shang S, Wang Y and Liu Z K 2007 *Appl. Phys. Lett.* **90** 101909

[22] Hill R 1952 *Phys. Soc.* **65** 350

[23] Miao N H, Sa B S, Zhou J and Sun Z M 2011 *Comp. Mater. Sci.* **50** 1559

[24] Zeng Z Y, Hu C E, Cai L C, Chen X R and Jing F Q 2010 *J. Phys. Chem.* B **114** 298

[25] Kresse G and Furthmuller J 1996 *Phys. Rev.* B **54** 11169

[26] Kresse G and Joubert D 1999 *Phys. Rev.* B **59** 1758

[27] Perdew J P, Chevary J A and Vosko S H 1992 *Phys. Rev.* B **46** 6671

[28] Monkhorst H J and Pack J D 1976 *Phys. Rev.* B **13** 5188

[29] van de Walle A, Asta M and Ceder G 2002 *Calphad* **26** 539

[30] Cynn H and Yoo C S 1999 *Phys. Rev.* B **59** 8526

[31] Dewaele A, Loubeyre P and Mezouar M 2004 *Phys. Rev.* B **70** 094112

[32] Li J H, Liang S H, Guo H B, and Liu B X 2005 *Appl. Phys. Lett.* **87** 194111

[33] David R Lide 2004 *CRC Handbook of Chemistry and Physics* 90th edn. (New York: CRC Press LLC) p. 787

[34] Gale W F and Totemeier T C 2004 *Smithells Metals Reference Book* 8th edn. (Oxford: Elsevier Butterworth-Heinemann) p. 15-3

[35] WooDs ADB 1964 *Phys. Rev.* **136** 781

[36] Featherstone F H and Neighbors J R 1963 *Phys. Rev.* **130** 1324

[37] Dwight E Gray 1957 *American Institute of Physics Handbook* 90th edn. (New York: American Institute of Physics) pp. 4–131

[38] Wu J H, Zhao X L, Song Y L and Wu G D 2011 *Int. J. Mod. Phys.* B **25** 1393

[39] Cohen R E and Gülseren O 2001 *Phys. Rev.* B **63** 224101

[40] Barin I 1995 *Thermochemical Data of Pure Substances* 3rd edn. (Germany: Verlagsgesellschaft bmH Weinheim) p. 1587

[41] Featherston F H and Neighbours J R 1963 *Phys. Rev.* **130** 1324

[42] Walker E and Bujard P 1980 *Solid State Commun.* **34** 691

[43] Wang Y, Wang J J, Zhang H, Manga V R, Shang S L, Chen L Q and Liu Z K 2010 *J. Phys.: Condens. Matter.* **22** 225404

[44] Zhang M, Yang B, Chu J and Nieh T G 2006 *Scripta Mater.* **54** 1227

[45] Kaye G W C and Laby T H *Tables of Physical & Chemical Constants Barometry* http://www.kayelaby.npl.co.uk/general_physics/2_4/2_4_1.html [2012-]